
Lithology and Fluids: Seismic Models of the Brushy Canyon Formation, West Texas

Michael Batzle and Michael H. Gardner, Departments of Geophysics and Geology and Geological Engineering, Colorado School of Mines, Golden, CO 80401

Abstract

Lithology and fluid information can be extracted from seismic data of deepwater clastics if their relative contribution to the signal is understood. Many factors combine to produce a seismic signature including stratal architecture, lithology, pore fluids, compaction, pore pressure, and near surface heterogeneities. Outcrop seismic models are constructed of the Brushy Canyon Formation along the Western Escarpment of the Guadalupe Mountains using rock and fluid properties from outcrop, normal and overpressured Gulf of Mexico and North Sea Basins to test seismic sensitivity to lithology, fluid, and pressure. Resolution is best in large, clean, gas-saturated, and over-pressured sandstones. Strong lithology contrasts improves resolution of km-scale sand bodies. Hydrocarbon saturation does not necessarily enhance seismic response. Lithology and fluid affects can reduce impedance contrast resulting in low amplitudes (dim spots). In contrast, elevated geopressures preserve porosity and produce low-velocities and high amplitudes (bright spots). Even in low impedance contrast sandstone and shale intervals, offset dependent amplitudes increase resolution and indicate hydrocarbons.

Introduction

Three-dimensional seismic surveys are the current primary exploration tool used for deepwater sandstone reservoir delineation. However, there are many uncertainties concerning what is actually being imaged. Because deep-water reservoirs occur in basins with different petroleum systems and depositional systems, it is often difficult to isolate the lithologic and fluid contribution to seismic response from variations related to architectural style. Despite these limitations, geologic models derived from seismic have become increasingly more robust as seismic resolution and 3D coverage has increases.

Seismic stratigraphy assumes reflectors follow chronostratigraphic surfaces and define genetic rock packages that comprise sequence stratigraphic models (e.g., Vail et al., 1977). In contrast, outcrop seismic models of a Permian carbonate shelf margin indicates that seismic reflectors more closely follow facies and facies-controlled property distributions (Stafleu and Sonnenfeld, 1994). These contrasting geologic interpretations of seismic data highlight the need for a better understanding of the controls governing the seismic response of stratal architecture.

Rock and fluid properties from different deepwater reservoir sandbodies produce extremely variable seismic expressions ranging from both positive to negative reflectors. The variability in reflector geometry, and in the interpretation of what it represents, reflects the multiple geologic variables that contribute to seismic response. The principle variables include:

- pore fluids
- reservoir pressure and depth
- spatial distribution of lithology and rock properties
- sandbody size and architecture of encasing nonreservoir strata.

These combine to determine seismic expression and reflect both the present reservoir setting and ancient depositional environment (Figure 1). In general, resolution is best when sand bodies are large and bounded by rocks of contrasting lithology (Figure 1). However, there are numerous exceptions to this generalization. Low sand/shale contrast can produce weak reflections and under some conditions even hydrocarbon saturation will produce low amplitudes (dim spots). This investigation models pore fluids, reservoir pressure, and lithology distributions that contribute to the seismic character of deep-water sandbodies.

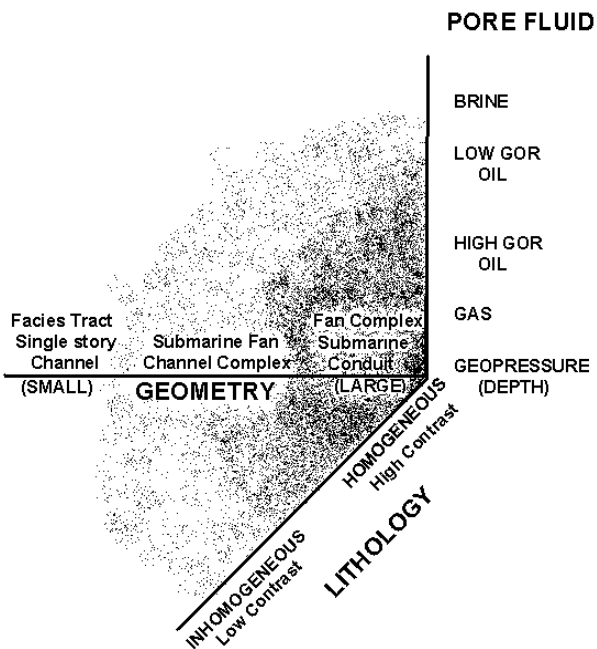


Figure 1. Chart summarizing the relative influence of lithology, fluid, and geometry on the seismic resolution of deepwater sandstone. The stippled region indicates optimum image area. Areas near the origin, in general, have the strongest seismic response.

Geologic Setting

Outcrops of the Brushy Canyon Formation expose an oblique depositional dip profile of deepwater sandstone and siltstone (Figure 2) exposed along an 80-kilometer outcrop belt (see Gardner and Borer, this volume). A seismic model is constructed across a proximal, siltstone-rich slope succession of low sand content (approximately 10%), dissected by clinoform surfaces modified by slumping. These clastic deposits thicken basinward to form a 400-meter thick clastic wedge deposited below the physiographic shelf margin.

Depositional patterns in this proximal setting are related to a stratigraphic hierarchy of seven submarine fans that stack to form the Brushy Canyon fan complex (Gardner and Borer, this volume). A conspicuous depositional pattern shown by this fan complex is an upward change from basin-centered to slope-centered sediment thicks (Figure 3). Basin-centered fans are 100-m thick, and slope-centered fans to the genetic top siltstone are 320-m thick at section M on the cross section. This thickness pattern reverses

30 km from the physiographic break, with basin-centered fans 250 meters thick and slope-centered fans 120 meters thick. Basin-centered fans onlap below the shelf break, are thin and generally sandstone-poor in slope facies tracts. Slope-centered fans onlap and fill submarine canyons, contain thick siltstone-dominated clinoform packages with large isolated sandstones in slope facies tracts. This reorganization in sedimentation pattern is defined by the 40 ft siltstone marker.

Architecture

The stratigraphic cross section used in the model is constructed from 24 regional stratigraphic sections tied to digital photomosaics and geologic maps (Figure 3). In outcrops proximal to the paleo-shelfbreak, deep-water clastics obliquely onlap an unconformity that floors submarine canyons incised into the underlying Leonardian carbonate shelf-margin. Sandstones and conglomerates fill erosional canyons and slope successions contain slump scar confined channel complexes (Gardner and Borer, this volume).

The lower Brushy Canyon consists of poorly resolved basin-centered fan deposits. Thin and siltstone-rich, fan 1-3 deposits onlap below the shelf margin. Fans 4 and 5 thin and merge by toplap that is indicated by the interbedded sandstone and organic-rich siltstone that form the middle part of the Brushy below the '40-ft' siltstone marker. Above this marker, clinoforms of slope-centered fans separate three, multistory channel complexes that rise stratigraphically basinward. Coalesced slump scars confine these kilometer-scale sandbodies encased in siltstone. Siltstones above these sandstones contain laterally continuous, organic-rich siltstones that correlate to back-stepping channel complexes that progressively onlap the margin northward along the outcrop. These organic-rich siltstones commonly drape discordances and clinoform surfaces and have the longest correlation lengths. They record periods of fan abandonment and form stratigraphic cycle boundaries at all scales.

The digitized seismic model includes: (1) Stratal surfaces separating rocks of different lithology, (2) formation boundaries and unconformities, (3) thin laterally continuous, organic-rich siltstone intervals, (4) channel sandbodies, (5) clinoform surfaces and (7) stratal discordances representing slump scars are. This simplified cross section is built to resolve larger

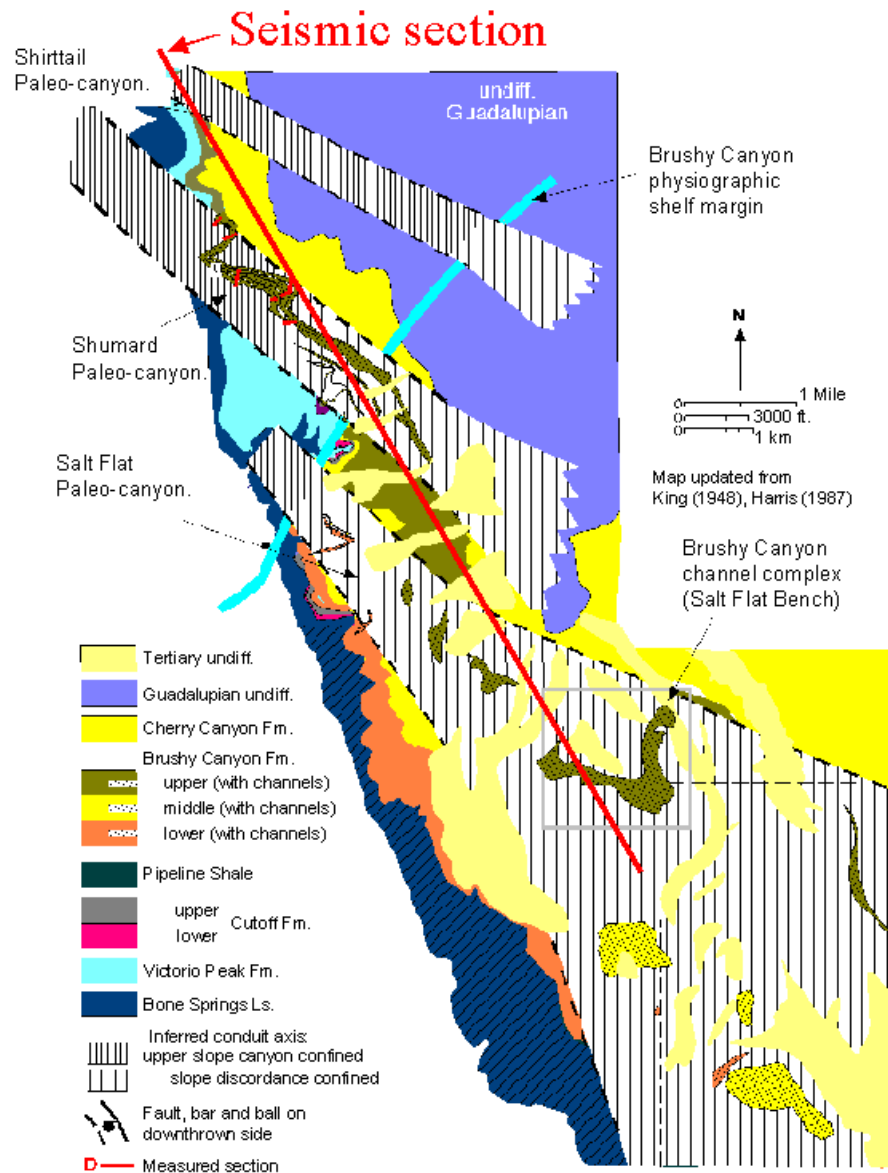


Figure 2. Inferred submarine conduits that obliquely intersect the outcrop belt of the Brushy Canyon Formation along the Western Escarpment of the Guadalupe Mountains. Location of modeled seismic cross section (Figure 4) is indicated by the heavy line.

seismic-scale features (Figure 4). Rock properties are held constant within each individual sediment body, but are varied spatially across the section by relating lithology to rock properties.

Rock Properties

Seismic impedance contrasts may be abrupt to gradual in a vertical sense, and continuous to discontinuous laterally. Velocity and density depend on

lithology, porosity, texture, and pore fluid. In general, high porosity yields low velocity and density.

Rock velocity data from the Brushy Canyon Formation was collected from core plugs along outcrop sections, and from well logs at Cabin Lake Field. Velocity distributions used to construct all seismic models are compared in Figures 5a, 5b, and 5c. In the three subsurface areas rock properties are derived from well logs.

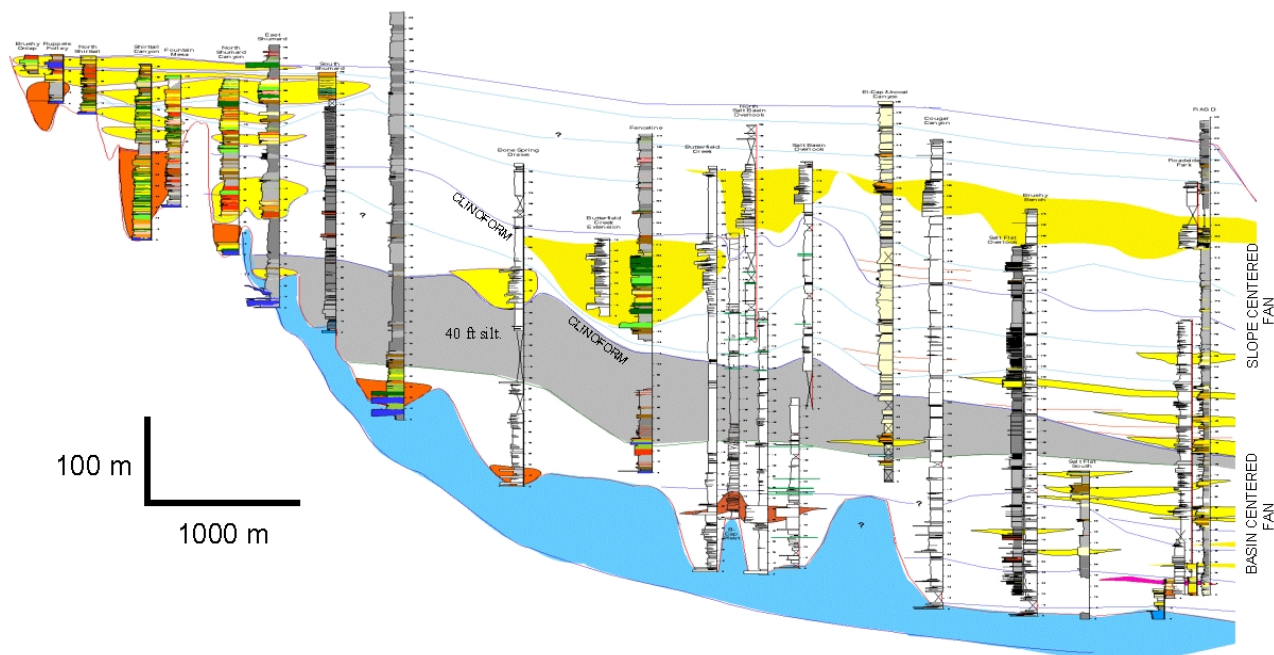


Figure 3. Simplified stratigraphic cross section showing the facies architecture through a proximal slope succession that onlaps a carbonate shelf margin. Cross section shows major sandbodies, clinoforms, stratigraphic cycle boundaries, and location of measured sections.

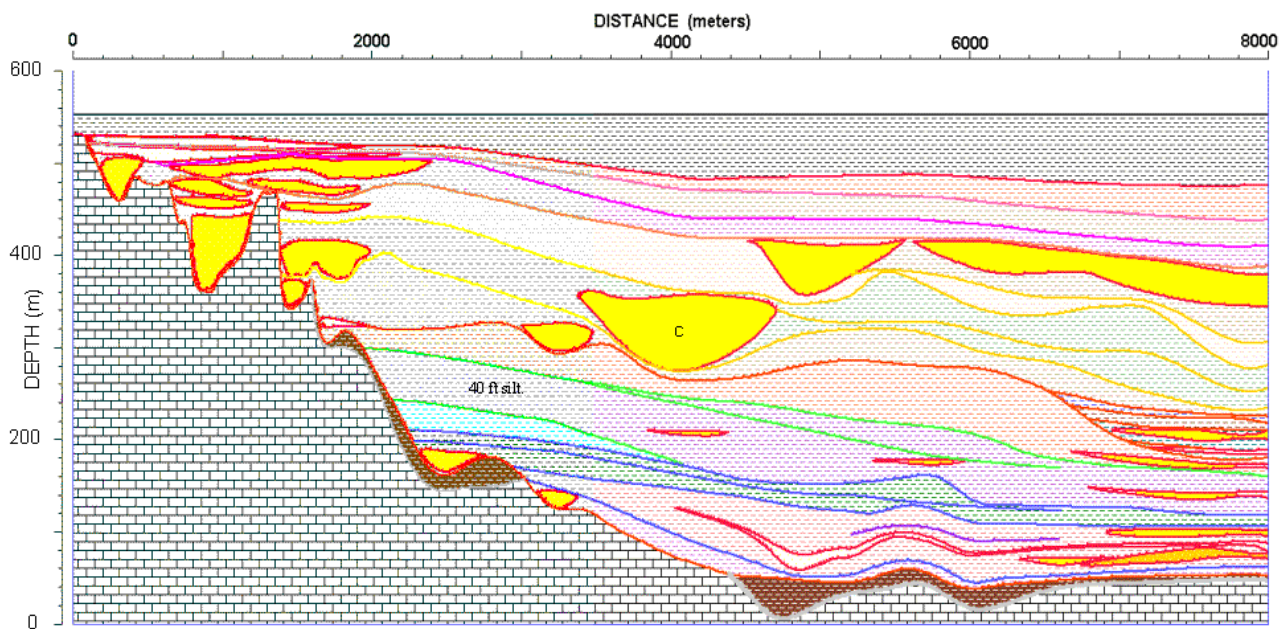


Figure 4. Digitized seismic model based on the geologic section in Figure 3. Sand body marked “C” is the focus of pore-fluid substitution calculations.

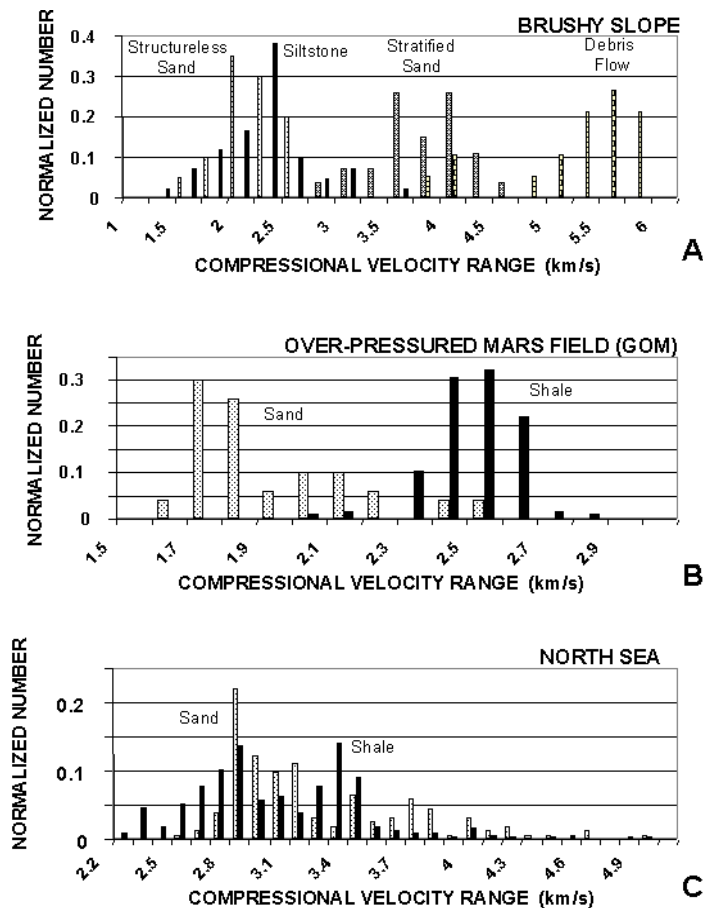


Figure 5. Normalized velocity distributions. (A): Brushy Canyon Formation velocity distributions. Siltstones (black) have velocities significantly lower than stratified sands and conglomerates, but can not be distinguished from structureless sands. (B): Shale and sand at Mars field. Despite the depth, geopressed sands have low velocity, significantly lower than encasing shales. (C): Normalized velocity distribution for the North Sea reservoir zone. Sand velocities are very similar to shale velocities. High velocity values indicate calcite cementation.

Principle facies within the cross section include:

- 1) Carbonate - The composition and pervasive cementation in carbonate rocks promote high velocities and densities. Limestone, dolomite, and megabreccia underlying deep-water clastics have very high velocities (5 to 6 km/s) and densities. Subordinate carbonate concretions in organic-rich siltstones and limestones below the 40 ft siltstone also show high velocities.
- 2) Sandstone and conglomerate - Very-fine to medium-grained sandstone is a well-sorted, subangular, subfeldspathic arenite. Structureless (2.3 km/s) and stratified sandstones (4 km/s) have porosities up to 15 % and the lowest velocity rock-seismic facies. Subordinate sandstone-matrix-supported conglomerates consist of carbonate clasts and allochems. These debris flows and carbonate clast-rich sandstone are well-cemented, dense and have the highest velocities (about 5.7 km/s).
- 3) Siltstone - Two siltstone types with varying organic content are present. Organic-poor siltstones are thinly interbedded to interlaminated with sandstones and form up to 200-m thick successions. Depending on sand content, these siltstones show a broad range of low to moderate velocities. Encasing siltstones average about 2.5 km/s and show strong impedance contrasts when in contact with stratified sandstone and conglomerate. However, siltstone is largely indistinguishable from structureless sandstone. Organic-rich siltstones contain thin carbonate concretions, volcanic ash beds altered to claystone, and have total organic carbon values ranging from 1-6% and higher velocities and densities. They form thin (< 3-m thick), laterally continuous, intervals that extend across the cross section.

Additional rock property data derived from well logs through the Brushy Canyon Formation at Cabin Lake Field in the northeastern Delaware Basin (Figure 6).

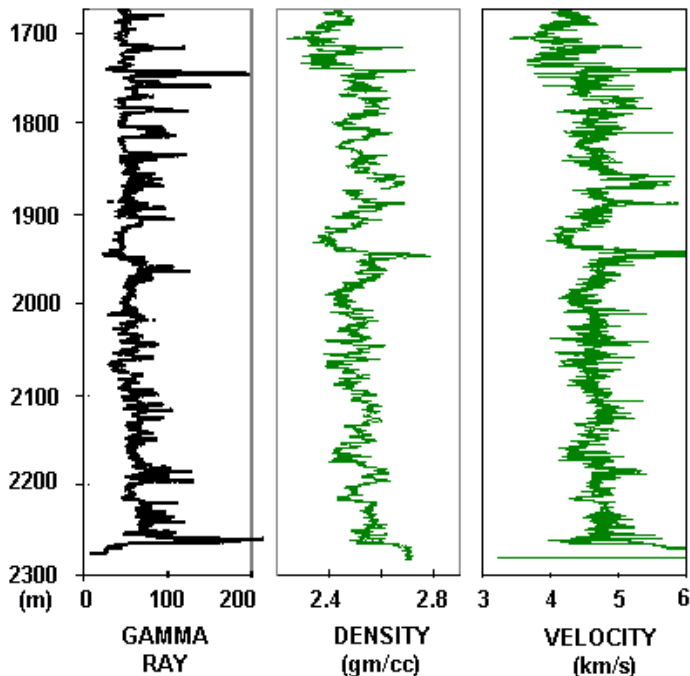


Figure 6. Gamma, density, and sonic logs from the Brushy Canyon Formation in the James A11 well, Cabin Lake Field, New Mexico. Thin, high API gamma ray zones are organic-rich siltstones. Increased cementation is indicated in sandstone in contact with organic-rich siltstones by increased density and velocity.

Although burial and diagenesis has produced more pervasive cementation, sonic and density logs show the same rock-seismic facies relationships documented in outcrop. Carbonates underlying the Brushy Canyon have high velocity, density, and impedance, which produces a strong basal reflection. Porous structureless sandstone has the lowest impedance (gamma-ray < 80 API). Siltstone and organic-rich siltstone have the highest gamma-ray values and show high impedance. Sandstones in contact with organic-rich siltstone are commonly cemented. The cemented sandstone and siltstone contacts produce the most consistent reflectors, with the organic-rich siltstone forming longest correlation length intervals.

Seismic Models

The stratigraphic cross section was digitized so that the architecture could be populated with different rock and fluid properties to assess their seismic response. Rock velocity and density vary with lithology and pore fluids to define seismic impedance. These properties do not necessarily correlate to a specific lithology, but their distribution produces impedance contrasts that define sandbody architecture. This architectural framework is held constant and lithology and fluid properties from three

deepwater provinces are substituted and related to seismic expression.

Synthetic sections from the digitized section are generated using the GXII software package. These models use normal incidence ray traces with first-order diffractions. The model is 0.6-km thick and 8-km in length (Figure 4) with a shot point separation of 80 meters. Traces are calculated and gain, frequency filter (wavelet), and noise are applied after ray paths and reflection coefficients are determined. A 40 Hz Ricker wavelet is applied to all models. An automatic gain control (AGC) is applied with 300 ms window. Noise at a -20 dB level is added to sections, band passed from 8 to 50 Hz.

Brushy Canyon Formation

The initial seismic model uses acoustic properties obtained from rock-seismic facies shown in Figure 5. These values are used to populate each layer or body in the model. Velocities and densities are varied within sediment bodies so that the stratal architecture shown in the cross section has seismic expression. Hence, the absolute amplitude of an individual reflectors should be viewed as a relative signature since a broad range of values can be applied to these sediment bodies.

Stratal architecture depicted on the noise-free cross section is apparent (Figure 7a). The strong reflection at the base is related to high impedance carbonates. The large slope sand bodies have strong positive reflections at their top, but strong negative reflections at their base because of the high impedance contrast with encasing siltstone facies. The ringing pattern in the lower right corner of the section is produced by the interbedded sandstone and siltstone that record the merging of the upper basin-centered fans. Subtle features within the thick slope-centered succession

are resolved in the noise-free model. Cliniform surfaces bounding fans that extend across the outcrop are resolved. Onlap of older deepwater clastics onto the basal unconformity is resolved and provides recognition criteria for resolving basin-centered fans. The organic-rich siltstone capping the Brushy Canyon fan complex forms a continuous reflector. Back-stepping channel complexes in slope-centered fans that onlap the shelf margin are poorly resolved. Noise is added to the section to mimic conventional data (Figure 7b).

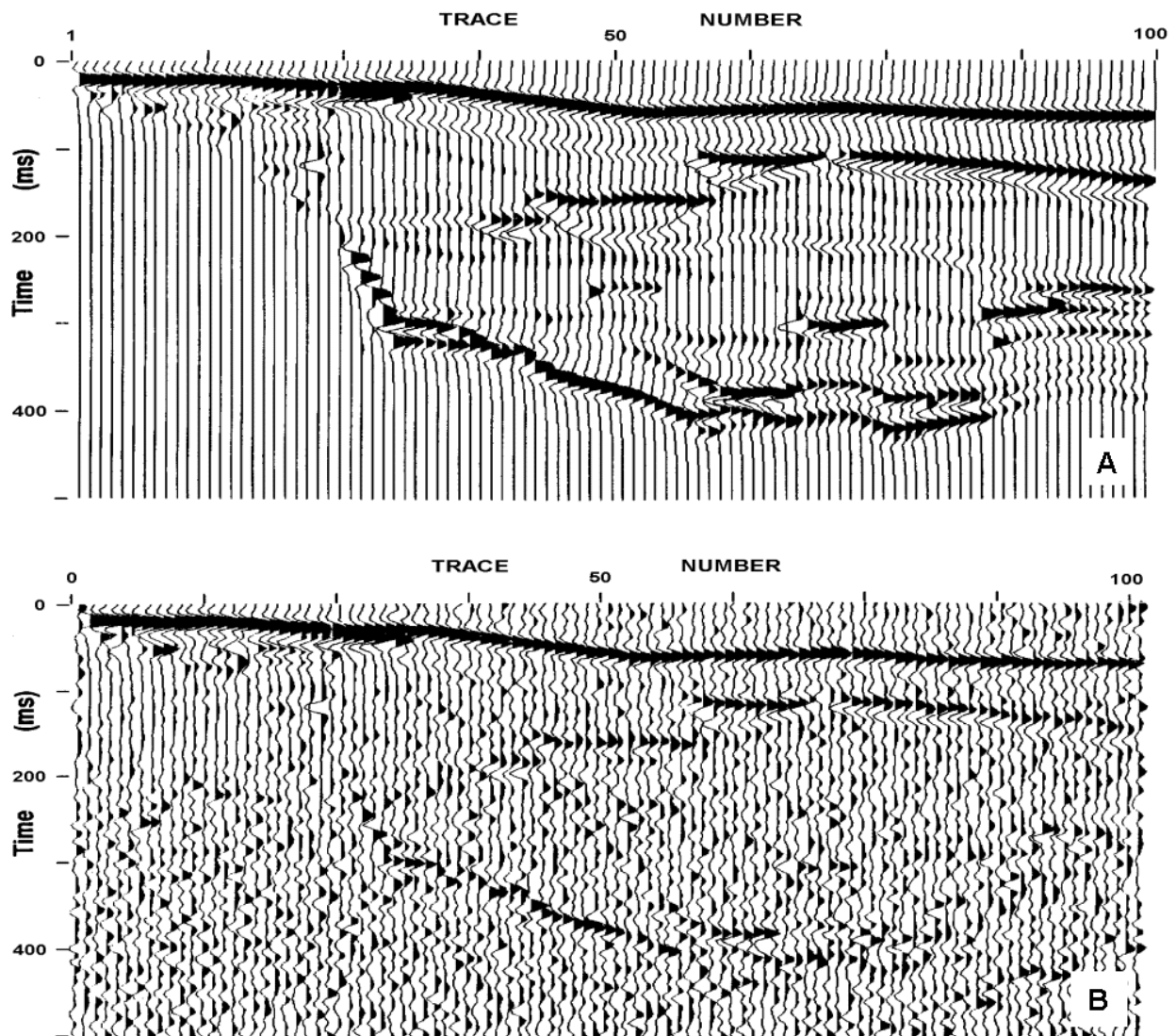


Figure 7. Seismic models for the Brushy Canyon Formation outcrop section (Figures 3 and 4) using measured Brushy properties. A zero-phase 40 Hz Ricker wavelet is used with an automatic gain control applied over a 300 ms window, (A): Noise-free, both sandbodies and cliniforms are resolved, (B): Same model with - 20 dB noise added. Cliniforms are still visible but difficult to trace. Sandbodies are apparent, but boundaries are difficult to detect.

Outcrop Model Case Studies

Our mapped architecture (Figures 3 and 4) forms the base case for substituting rock properties from three other deepwater reservoir settings. Two examples are from the mud-rich Mississippi fan complex. These are compared with sand-rich fan complexes in the Paleocene fill of the North Sea Basin. Two examples representative of deeper burial GOM deep-water reservoirs are examined; these settings contain normal and overpressured deepwater reservoirs.

Normal-Pressure, Gulf of Mexico Reservoirs

Sandstone and shale properties vary widely in the Gulf of Mexico (GOM) Basin. Reservoir sandstones have velocities that may be higher and lower than enclosing shale, which can produce a positive, negative, or no reflection. Figure 8 shows the general trend for normally-pressured Miocene sandstone and shale in the GOM (Gardner et al., 1974).

Offshore Louisiana contains a thick Tertiary succession of relatively unconsolidated sediment. In the South Marsh Island area, shelf sandstone are channelized and pond behind subtle topographic highs of deeper salt domes. Brine-saturated sandstone at moderate depths (about 500 to 1500 m) have lower compressional velocities and impedance than shale (Figure 9). Hydrocarbon saturation increases the velocity contrast at shallow depth. With increasing depth, however, this relationship changes and sandstone can have a higher compressional velocity than

shale (Figure 10). At greater depths hydrocarbon saturation decreases sandstone density and velocity. This brings sandstone density and velocity closer to shale and eliminates the reflection.

The seismic model uses deeply buried but normally pressured GOM rock and fluid properties (see Figure 10). Sandstone is populated with GOM sand properties and shale properties are substituted for siltstone and carbonate facies in the model. This produces a much smaller contrast and subdued boundary reflection at the basal unconformity (Figures 11 a and b). Channel complex sand bodies reflectors, however, resemble the model using outcrop properties. The ringing signal due to topset thinning in the lower right and onlap thinning in the upper left portions of the section are apparent. Reflectors representing the back-stepping channel complex in the upper left of the model are enhanced because of the reduced amplitude of the uppermost reflector. Reflection characters and overall sedimentary geometries are still visible when noise is added (Figure 11 b). This enhancement is partly because strong reflectors reduce muting caused by automatic gain control (AGC). In addition, lower overall velocities result in a relative time stretch, which has an effect of increasing the frequency.

The influence of hydrocarbons on seismic resolution is assessed through simple fluid substitution. Velocities for typical brine-saturated sandstone are slightly greater than surrounding shales at normal pressures

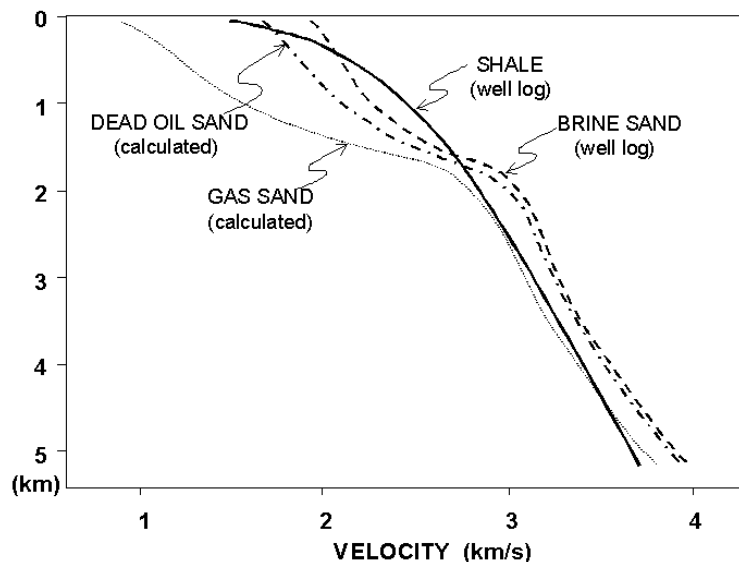


Figure 8. General sand-shale velocity relationships for the Gulf of Mexico under normal pressure conditions (Gardner et al., 1974). At depths below about 1700 m, shales have higher velocities than brine sands. Below this depth, brine-saturated sands are generally faster.

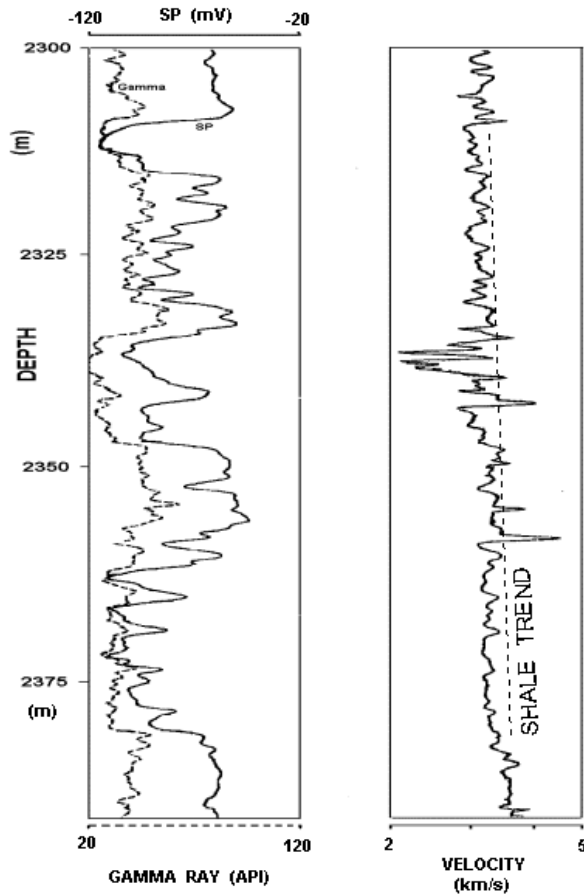


Figure 9. Gamma ray, SP, and sonic logs through a shallow, brine-saturated sand on the continental shelf, offshore Louisiana. These sands have lower velocity than adjacent shales and hydrocarbon saturation would increase this velocity difference.

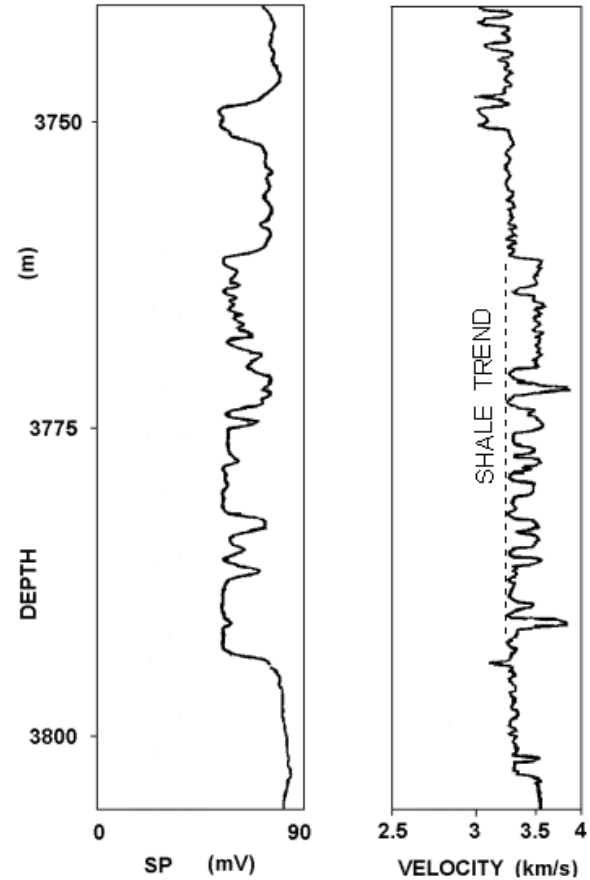


Figure 10. Gamma ray, SP, and sonic logs through a deep, brine-saturated sand on the continental shelf, offshore Louisiana. Brine sands have higher velocity than adjacent shales and hydrocarbon saturation would reduce this velocity difference.

for this depth (Figure 10). Either gas or light, high gas-oil ratio (GOR) oils decrease sand velocity and density almost to the level of encasing shale. Reducing the impedance contrasts produces a “dim spot,” or low-amplitude reflector. This is illustrated by sand body “C” (outlined, Figure 12a), which was resaturated with hydrocarbons in another model run (Figure 12a and b). The sandbody top reflection is a weak “dim spot” when compared to adjacent brine-saturated sandstone. This hydrocarbon indicator is the opposite of “bright spots” that develop shallower in the section, where low velocities of brine-saturated sandstone are further reduced by hydrocarbons.

Overpressured Gulf of Mexico

To assess the effect of geopressure or high pore pressures, a seismic model was constructed using properties from reservoir sandstones buried to 3.5-km depth at Mars field, in Mississippi Canyon block 803 (Figure 13; Chapin, et al., 1996). As in the last example, both siltstone and carbonate are replaced with shale velocities (Figure 12).

The combination of overpressure and minimal diagenesis preserves high porosities in sandstones of very-low density, velocity and impedance. In this case, sand densities and velocities are further de-

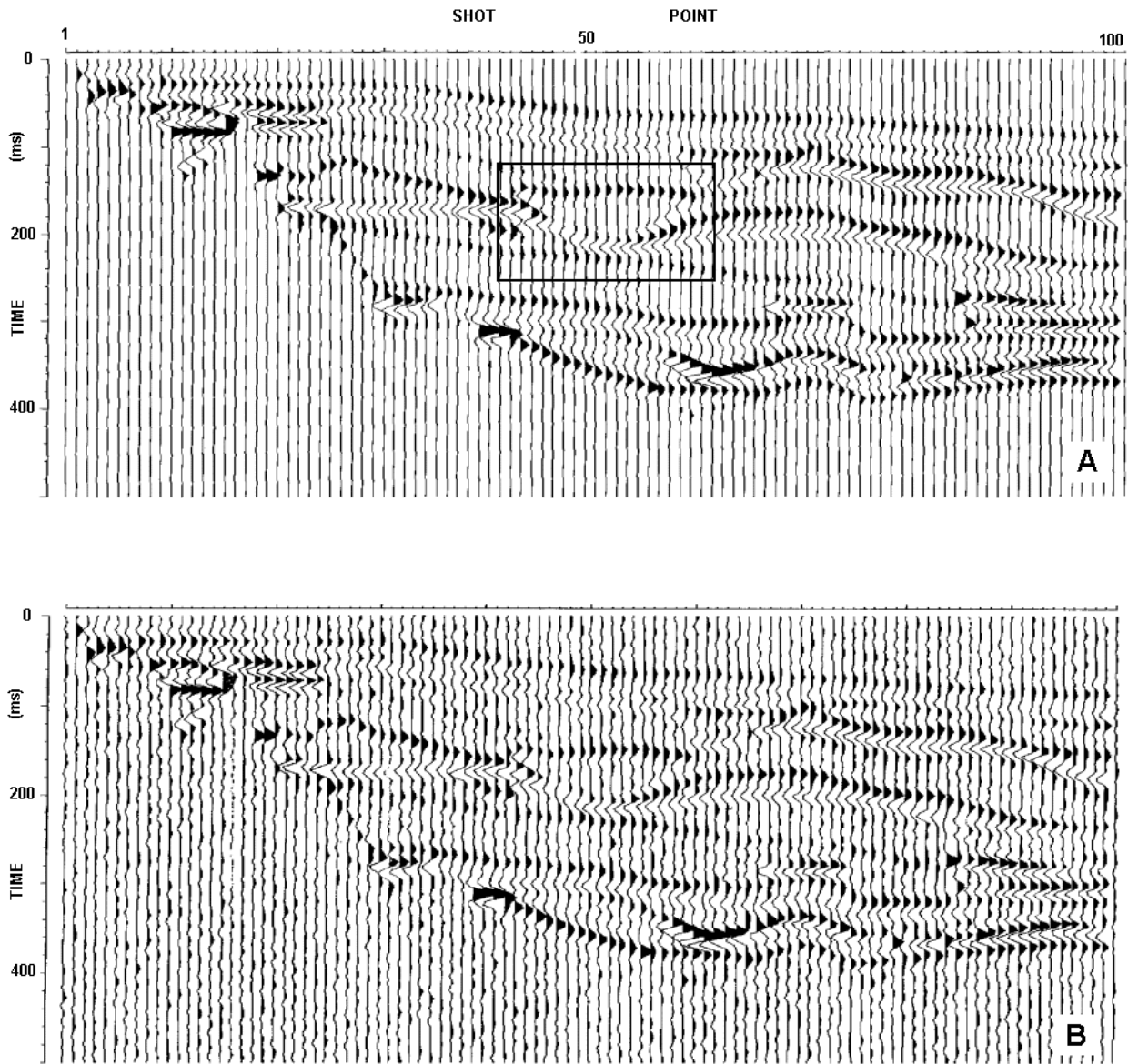


Figure 11. A seismic model using deep, normally pressured Gulf of Mexico rock properties (Figure 10), (A) Noise-free, Note that sand ‘C’ (outline) is still clearly visible and slower velocities have stretched the image in two-way transit time, (B) - 20 dB noise added.

pressed because of saturation by a high GOR oil. The high velocity contrast between shale and sandstone, and the overall low velocities are distinctive (almost the same as pure water 1.5 km/s, see Figure 13), and out of alignment with burial pressure trends (Figure 8). The overpressured sandstone velocities (1.8 km/s) are substantially lower than those of the encasing shale (2.6 km/s). This produces a large negative contrast between the reservoir sandstone and encasing shale, and produces a strong bright spot even at great depths.

A strong contrast between shale and sandstone produces very strong reflections. Sand body “C” is populated with hydrocarbon-saturated sandstone velocities (Figures 14a and 14b). Sand body reflections are strong and easily discernable even in the noise-added seismic section. Since a seismic wave takes longer to pass through these low-velocity rocks, sand bodies are stretched in time and internal channel architecture is resolved. The sand bodies are ‘bright’ at depths that under normal pressures would produce subdued reflections (see Figures 11 and 12). Brine-

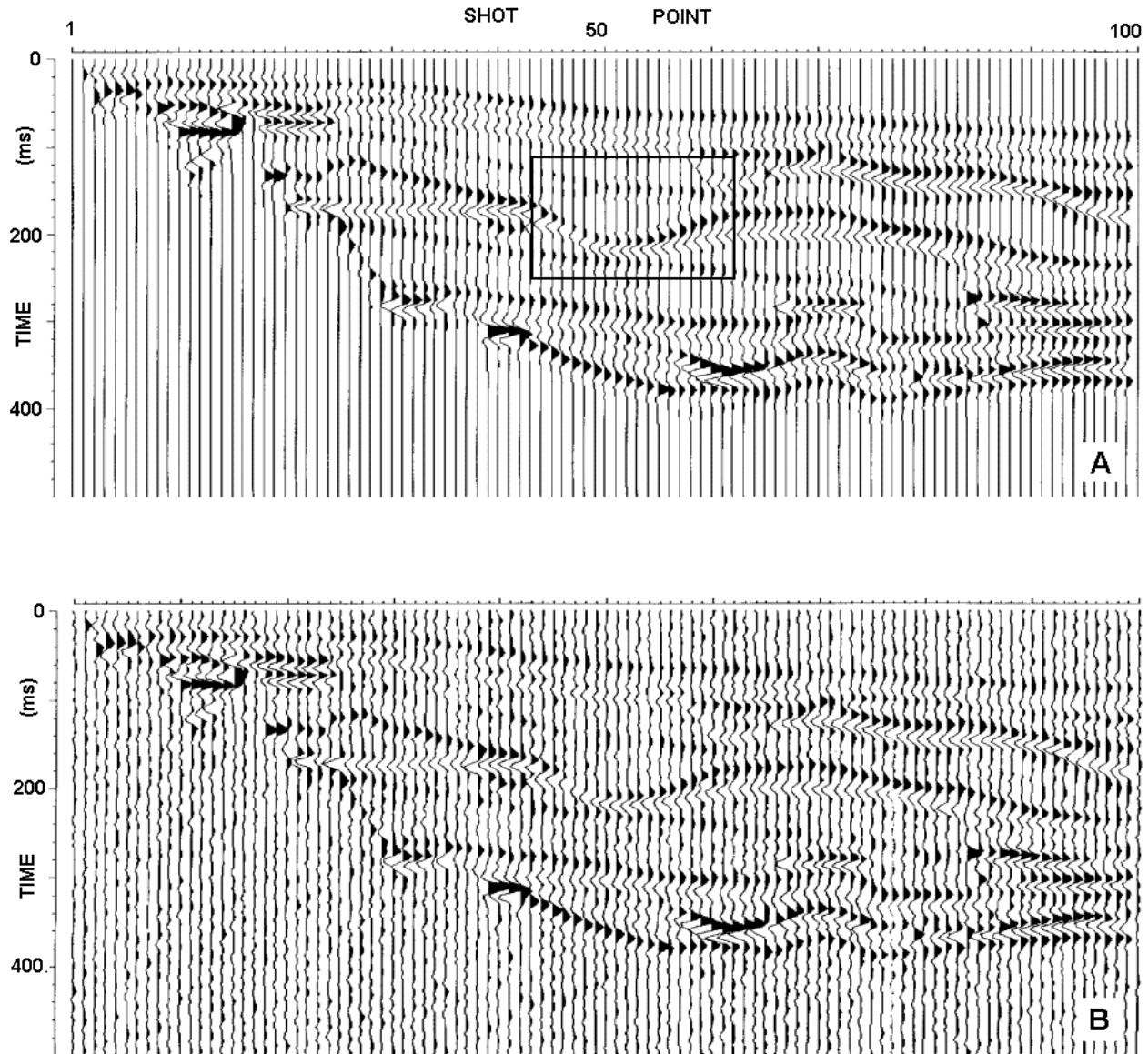


Figure 12 A seismic model for using deep, normally pressured Gulf of Mexico rock properties except with a light oil saturating the outlined sand, (A) Noise-free. Reduced velocities in this sand at normal pressured conditions have reduced the reflection coefficient. A 'dim spot' results. (B) - 20 dB noise added. With increased noise, this oil channel sand is no longer detectable. The reflection appears to be a continuation of the siltstone internal clinoform.

saturated sand bodies also have higher velocities and also show strong reflections, so that amplitude can not be used to distinguish brine- from gas-saturated sandstone.

North Sea Basin

The North Viking Graben contains thick, sand-rich, Paleocene deepwater clastics (Keys and Foster, 1996). These sandstones and shales have almost

identical velocity distributions (2.6 to 4 km/s; Figure 5c). Compressional (V_p) and shear (V_s) velocity logs show little contrast between sandstone and shale (Figure 15). The strongest reflectors are produced by high density and low porosity carbonate-cemented sandstone. These cemented zones and calcite stringers produce the strongest impedance contrasts, and inhibit direct sand detection. Hence, the maximum impedance contrast is commonly not at sandstone/

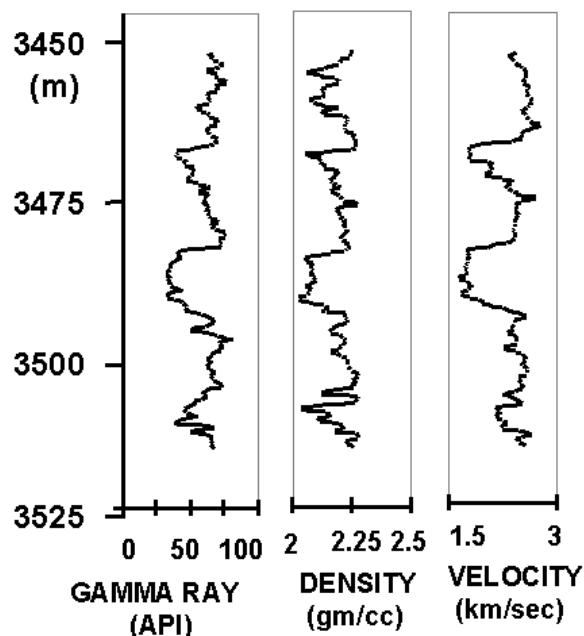


Figure 13. Gamma ray, density, and sonic logs through the deepwater reservoir sands at Mississippi Canyon block 803, Mars Field (after Chapin et al., 1995). These hydrocarbon saturated sands have very low density and velocity despite the depth due largely to geopressure and lack of diagenesis.

shale contacts. These high velocity, calcite-rich lenses are represented by alternating high and low impedance beds in the upper onlap and middle toplap areas of seismic model.

In high-velocity sandstone, resolution is reduced because transit time is contracted through the channel sand body. Reflections of channel sand bodies are also muted because of the lower velocity contrast with encasing shale. Consequently, discrete channel complexes are represented by a single wavelength, and reflection amplitudes are inconsistent and both negative and positive. Hence, sand body architecture is difficult to distinguish in this setting even when hydrocarbon saturated (Figure 16 b).

We can expand this analysis to include seismic attributes that detect the presence of hydrocarbons. Amplitude versus offset (AVO) analysis of a prestack seismic gather looks for changes in compressional reflection amplitude as a function of distance from the source. Reflection amplitude depends on compressional and shear velocities (V_p , V_s) and the incident angle of the seismic wave. Hydrocarbon-

bearing sandstone at 1980-m depth show opposite responses on the V_p versus V_s logs: V_p drops as V_s increases. A decrease in V_p/V_s ratio increases the far offset (or large angle) reflection amplitudes. Since hydrocarbons drop V_p but leave V_s unchanged, the V_p/V_s ratio decreases in hydrocarbon-saturated sandstones and produces an increase in AVO. A calculated prestack gather using GOM logs (Figure 10) is shown in Figure 17. The reflector above 2000 ms shows a strong amplitude gain, with offset from left to right. The actual common midpoint gather (CMP) from this location shows a strong AVO response (Figure 18; leftmost traces are strongest). Near-trace far-trace subtraction techniques resolve gas-saturated sandstone from noise in the section.

Discussion

Comparison of these various seismic models demonstrate the strong control that lithology, pore fluid, depth, and pressure have on seismic signature. These physical factors combine to control the resolution of deepwater sand bodies (Figure 1). The brighter, red-shaded region in Figure 1 indicates the optimum conditions for resolving sandbodies. Figure 1 show that large, clean, gas-saturated, and over-pressured sandstone has the highest resolution. Low sand/shale contrasts produce weak reflections and hydrocarbon saturation that can produce low amplitudes (dim spots). Velocities and impedances are lower in sandstone saturated with gas, or light, high gas-oil ratio (GOR) oils. Reservoir pressure has a dramatic effect on seismic resolution. Higher than normal pore pressures often arrest compaction and produce abnormally high porosity sandstone at great depths.

Scale is another important factor governing seismic resolution. Although often mapped and termed channels, the seismically resolvable channel form feature in all models is a compound sand body consisting of deposits recording multiple depositional events. The size of these slope channel complexes reflects their confinement within a larger depression and does not represent the scale of the depositing flow. Hence, relating facies scale depositional processes to seismic-scale bodies is considered untenable.

Seismic resolution of deep-water architecture is also dependent on the noise-level produced by surface heterogeneities. When noise is added, to mimic conventional data, the effect lowers the resolution of

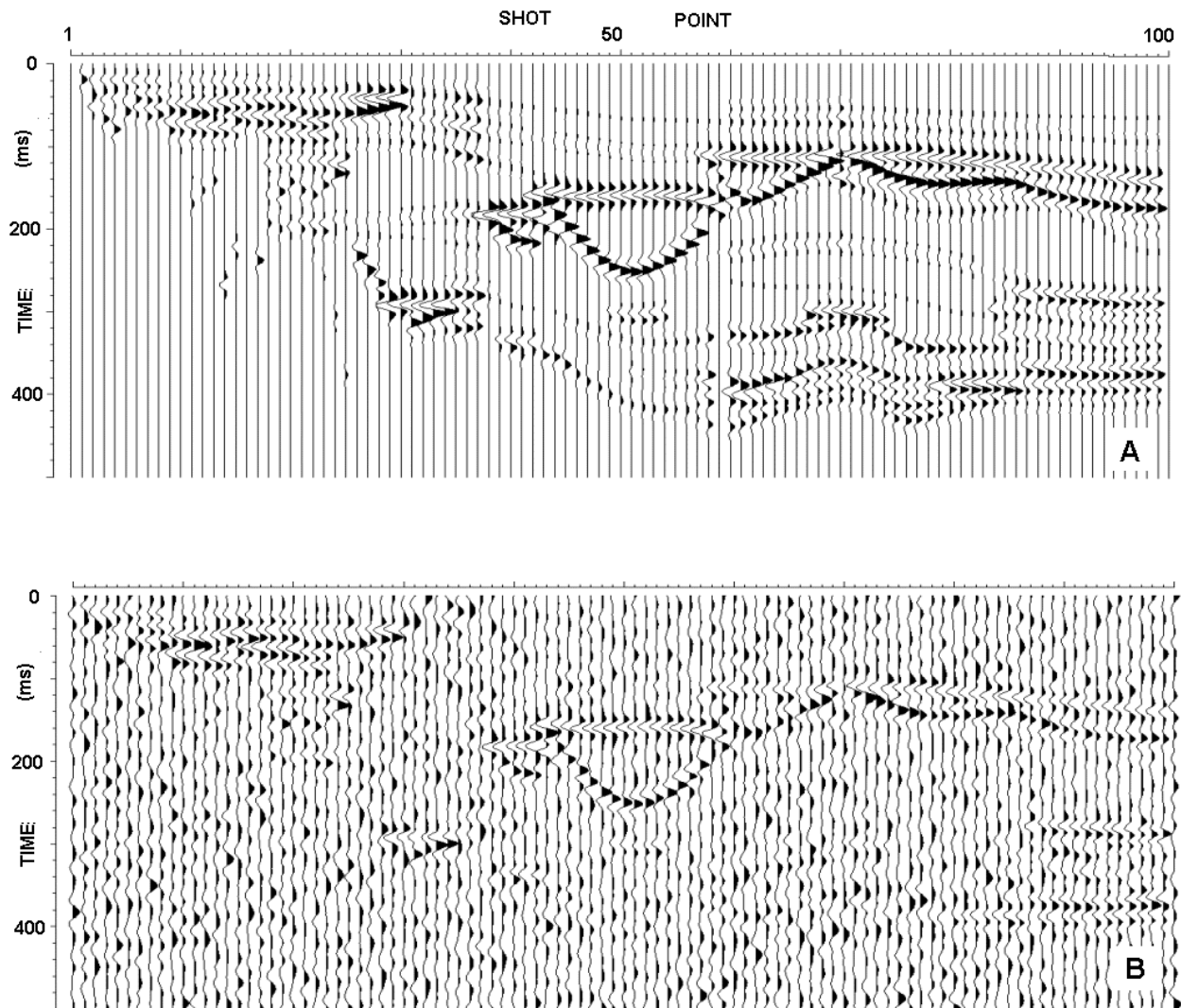


Figure 14. A seismic model using deep, but overpressured Gulf of Mexico rock properties from the Mars Field (Figure 5b), (A): Noise-free. Low velocities and high impedance contrasts make the sand bodies obvious. Because of the low sand velocities, the reflection has reversed sign (now negative) and the channel is significantly stretched in time. (B): - 20 dB noise added. Despite increased noise, sand is easily detected.

individual sandbodies (Figure 7b). For example, the correlation of isolated sandbodies shown in Figure 7b seems plausible. The feature at shot point 60 might erroneously be interpreted as a fault displacing sandstone about 60 ms to the left. This interpretation is supported by an apparent similar offset in the lower reflector at 360 ms. Such an interpretation would predict a reservoir that is compartmentalized by faults. The alternative and correct interpretation shows sandstone architecture related to the stratigraphic stacking pattern of deep-water channel complexes in a prograding slope succession.

Conclusions

Seismic response for deepwater clastic can vary substantially, ranging from bright positive or negative reflections, to nearly invisible. Primary factors include: (1) size and geometry, (2) lithology and property contrast, (3) pore fluids, and (4) pore pressure. Signal frequency content, seismic velocity, and internal sand body structures will modify expression. The impedance contrast with the surrounding lithologies determines the magnitude of the reflection but is not constant or simple for the same lithologies. Hy-

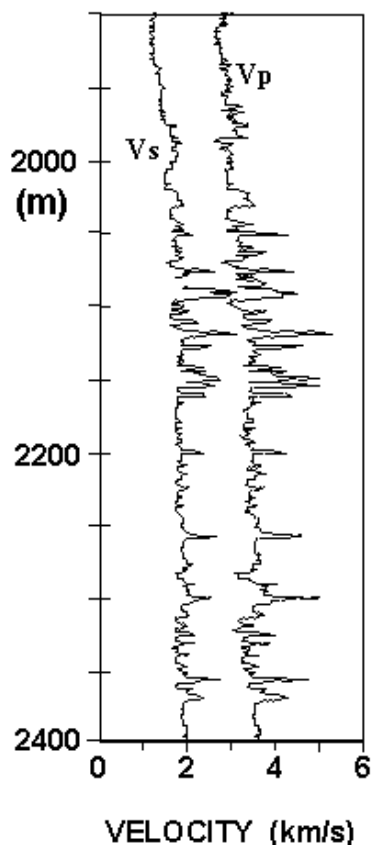


Figure 15. Compressional and shear logs through a Paleocene deep-water reservoir in the Viking Graben, North Sea Basin (Keys and Foster, 1998). The sandstone reservoir starts just above 2000 m depth and shows a drop in compressional velocity but a slight increase in shear velocity.

drocarbon saturation lowers sand impedance, but reflection strength may weaken depending on the properties of the surrounding material. Increased pore pressure generally increases sand body reflections and enhances the hydrocarbon response.

Acknowledgments

Support was provided by members of the Resource Optimization of Slope and Basin Reservoirs Consortium members: ARCO Exploration & Production Technology, Amoco Production Company, British Petroleum, Conoco Inc., Elf Exploration Production, Exxon Production Research Company, Marathon Oil Company, Mobil Exploration and Producing Technical Center, ORYX Energy Company, Phillips Petroleum Company, Shell Offshore Inc., Statoil,

Texaco Exploration and Production, Inc., and Unocal Corporation.

Mark Sonnenfeld helped conduct fieldwork and Brad Sinex assisted in building the first seismic models. Phillips Petroleum provided subsurface data from Cabin Lake Field. Mr. Fred Armstrong, Resource Manager at Guadalupe Mountains National Park, was extremely helpful in providing logistics support and park permits to conduct this work.

References

- Chapin, M. A., G.M. Tiller, and M.J. Mahaffie, 1996, 3-D architecture modeling using high-resolution seismic data and sparse well control: an example from the Mars "Pink" reservoir, Mississippi Canyon area, Gulf of Mexico; *in* P. Weimer and T.L. Davis eds., AAPG Studies in Geology 42, and SEG Geophysical Development Series 5, AAPG/SEG Tulsa, p.123-132.
- Gardner, M.G., and Borer, J, in press, Submarine channel architecture along a slope to basin profile, Brushy Canyon Formation, West Texas. A. Bouma (ed.) Fine-Grained Turbidite Systems. (this volume)
- Gardner, G.H.F., L.W. Gardner, and A. R. Gregory, 1974, Formation velocity and density - the diagnostic of stratigraphic traps: *Geophysics*, v. 39, p. 770-780.
- Keys, R. and D. Foster, 1998, Comparison of seismic inversion methods on a single real seismic data set (1994 open workshop results); Society of Exploration Geophysicists, in press.
- Staffeu, J., and M.D. Sonnenfeld, 1994, Seismic models of a shelf-margin depositional sequence: upper San Andres Formation, Last Chance Canyon, New Mexico: *Journal of Sedimentary Research*, v. B64, p. 481-499.
- Vail, P.R., R.M. Jr. Mitchum, R.G. Todd, J.M. Widmeir, S. Thompson III, J.B. Sangree, J.N. Bubb, and W.G. Hatlelid, 1977, Seismic stratigraphy and global changes of sea level *in* C.E. Payton ed., *Seismic stratigraphy – applications to hydrocarbon exploration*, AAPG Memoir 26, p. 49-212.

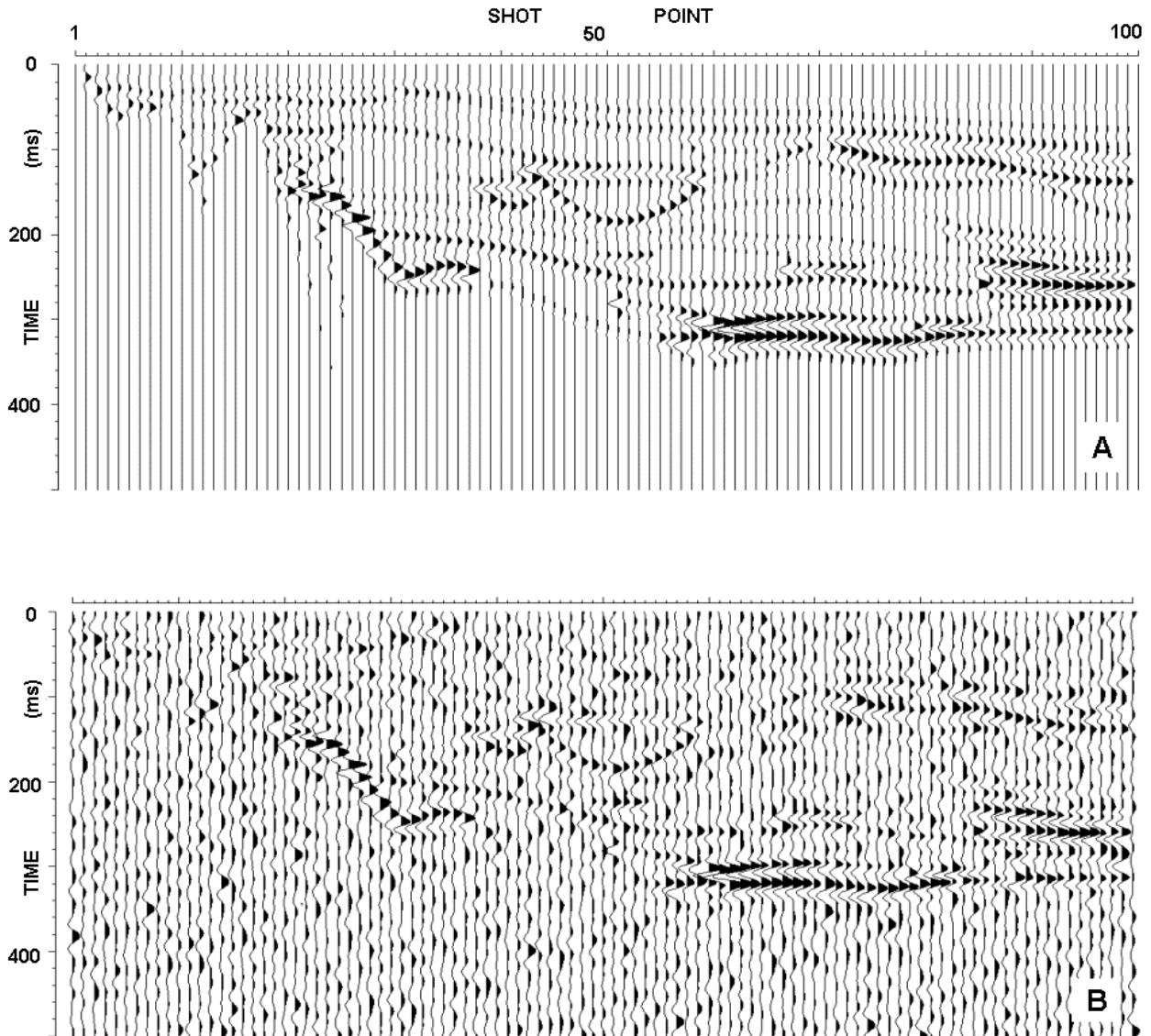


Figure 16. A seismic model with North Sea rock properties (Figure 5c). Sands and shales have similar impedances and sandbody reflections are weak. (A): Noise-free, the strongest reflections arise from carbonate-rich beds represented in the lower right of the model, (B) - 20 dB noise added. Sandbodies are difficult to distinguish from background shale. Different attributes, such as amplitude versus offset are needed.

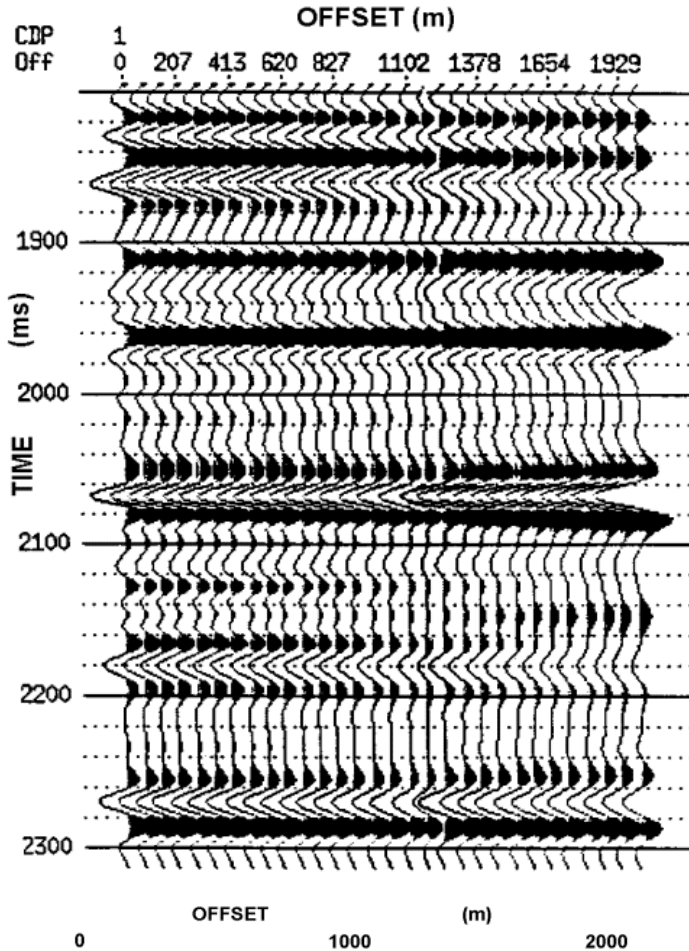


Figure 17. Modeled prestack gather based on the North Sea velocities (Figure 15). Just above 2000 ms, a strong increase in amplitude with offset is seen.

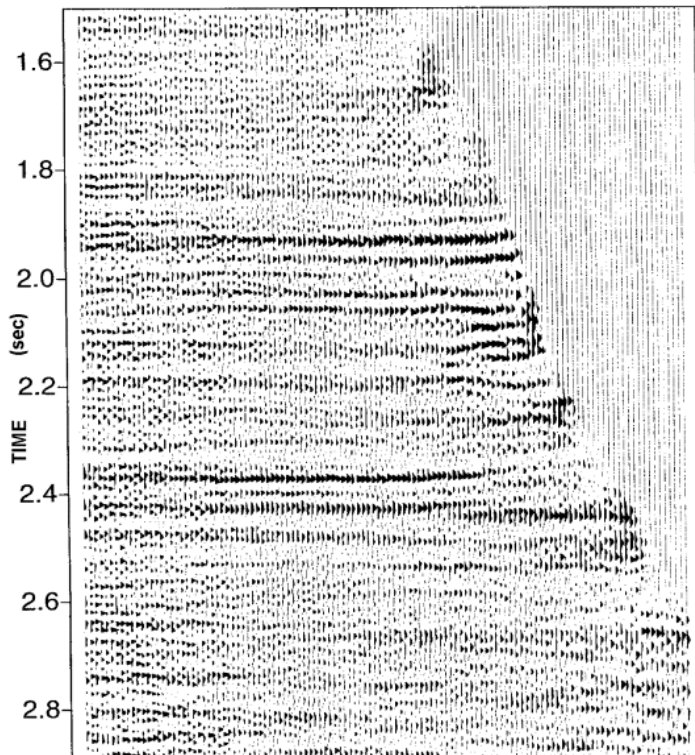


Figure 18. Prestack common midpoint gather (CMP) recorded at the North Sea well location (Keys and Foster, 1998). Although the typical stacked reflection was weak, this hydrocarbon saturated deepwater sand (above 2000 ms) does give a strong amplitude versus offset signature.